Posted: October 12, 2023

CLING-ERS: A Mechanism for Autonomous In-Orbit Rendezvous and Docking

Melodie R. Ebrahimi[1] and David A. Barnhart[2]

[1]Marlborough School, 250 South Rossmore Avenue, Los Angeles, CA 90004
[2]Department of Astronautical Engineering, University of Southern California, Los Angeles, CA 90007, United States

Abstract

Spacecraft Rendezvous Proximity Operations and Docking (RPO-D) is a critical function to enable endless applications in space; spacecraft servicing, orbital refueling, spacecraft repair/upgrade and manufacturing in space are just some of the applications. For these applications to occur at scale, a system must be able to "connect things" that are low weight, low cost, and have a developed computationally efficient algorithm for final dock/connect. Currently in space-to-space interactions there is not a consensus between customers, operators, manufacturers and users on a "standard" means of connecting space objects. The USC SERC created CLING-ERS as a standalone device to address a ubiquitous docking mechanism for in space interactions. CLINGERS combines a traditional mechanical interconnected with a relative navigation algorithm using Perspective-n-Point (PnP) to solve the pose estimation problem between space elements enabled with CLINGERS. Ideally any spacecraft/platform mounted with a CLING-ERS device could use its embedded navigation sensor information for autonomous docking with another object mounted with a CLING-ERS unit.

Keywords— Rendezvous and Proximity Operations, Rendezvous Proximity Operations and Docking, CLING-ERS, Perspective-n-Point, Autonomous Docking.

1 Introduction

1.1 CLING-ERS: A Mechanism for Autonomous In-Orbit Rendezvous and Docking

A genderless docking mechanism was created and patented by a USC professor (Dr Berok Khoshnevis) to support ground robotics. CLING or Compliant Low-profile Independent Non-protruding Genderless system, was created in order to explore a genderless docking mechanism versatile for ground robotics. The CLING basic design can be seen in 1. As safety of rendezvous in Space operations became more apparent with new space servicing applications, SERC (Space Engineering Research Center) initiated some research with the Aerospace Corporation to merge the original CLING concept with functions of close in sensing and ranging. CLINGERS (7) was then created with Electronic Rendezvous Sensors as a merger between the traditional "Docking" mechanism and "RPO" sensing systems(8). Early prototypes had CLING mechanical devices coupled with simple LED lights that were used to determine pose (orientation), and tested (2 on an air bearing table to simulate space-like conditions in a single plane. These tests gave excellent results in 2D.

CLINGERS is on track to be tested in full 6 DOF (Degrees of Freedom) in the microgravity robotic research platform inside the ISS. This testing in June of 2023 will be using NASA Ames Research Lab's Astrobee(9) (cube-shaped robots that move in microgravity) free flight modules. The two CLINGERS will be attached to separate Astrobee's 3a, where they will dock in 3D 3b, utilizing internally developed PnP (Perspective-n-Point) algorithm that allows the pinpoint of LEDs on the CLINGERS which then transmit pose and range information (orientation and distance) to the Astrobee hosts that then can rotate and translate to the other CLINGERS to prove docking.

CLING-ERS is USC and SERC's first project to be sent to the ISS, and it will uncover a new dimension in micro-docking systems that can extend to larger scale efforts under inspection, servicing, assembly and manufacturing (ISAM). The CLING-ERS genderless mechanism, utilizing a PnP algorithm, will be more efficient and versatile than existing mechanisms, and could be used on almost any object in space. Despite the intense focus on a P3P solution (three points of reference) with a gendered docking system, few researchers have examined a Nakano inspired PnP solution that uses four points to find the one "true solution" (for rotation and translation matrices) and an OpenCV (Open Source Computer Vision Library) PnP algorithm, along with a genderless autonomous docking system that fits in a small, small, non extruding, autonomous and genderless docking mechanism. If successful, CLINGERS will provide flexibility for

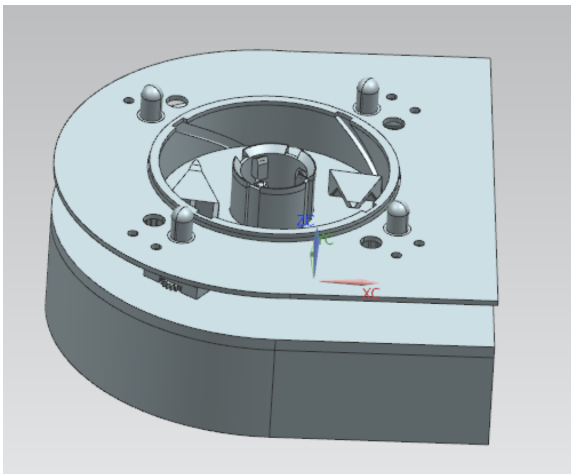

Figure 1: Computer Aided Design Model: CLING.

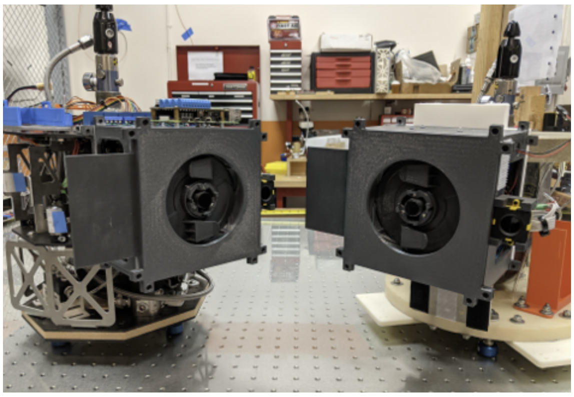

Figure 2: The CLINGERS mechanism was tested while attached to FloatBots, which utilize cold gas thrusters to frictionlessly move across the SERC's air-bearing table.

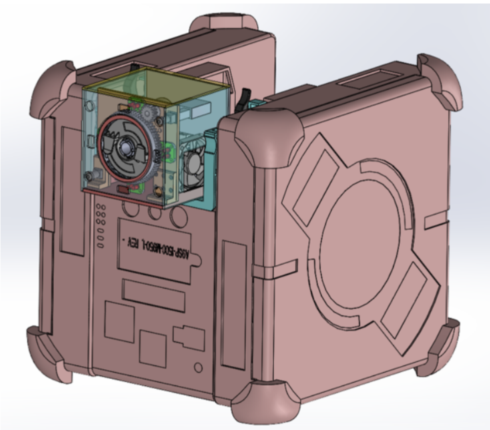

(a) CAD: CLINGERS module integrated on the Astrobee.

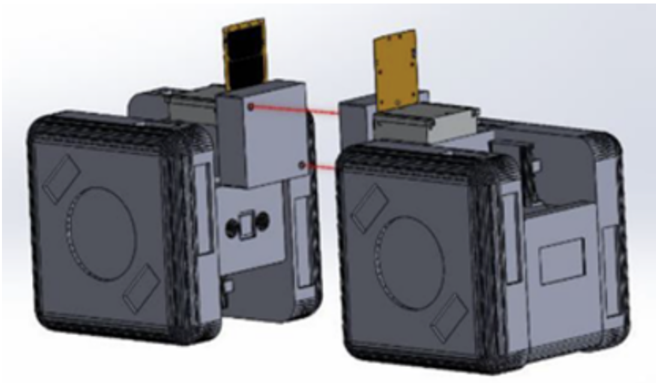

(b) ISS engagement and sensing.

Figure 3: CLINGERS module and ISS engagement

engineers to approach and consider docking systems for large scale assembly in space. It will also increase overall accuracy and safety in RPO (Rendezvous and Proximity Operations) scenarios, allow for a semi-standard (mechanical equipment standard) docking methodology, and an optimized capture mechanism (passive capture technique) and algorithm.

1.2 Space Autonomous Docking

Autonomous docking is the autonomous function required for two spacecraft at remote distances to come together and contact, without impact. The process between the two objects is as follows: achieving a common orbit, rendezvousing with one another from distance, contact then dock (hard connect), and control of the new combined-space element (i.e. two space systems now connected) in orbit and attitude.

Autonomous docking research has been done (Wertz and Bell, 2003) (20) to analyze the status and prospects of autonomous rendezvous and docking. In 2003, James R. Wertz and Robert Bell realized that this process requires the development and testing of many new technologies, from absolute and relative autonomous navigation, to hardware and software of sensors and actuators. Autonomy allows for potentially lower costs, risk reduction, and new mission modes.

Research has also been done (Philip and Ananthasayanam, 2003) (17) in regards to relative position and attitude (position in 3D space) estimations, as well as control schemes for the final phase of an autonomous docking mission of a spacecraft. Outputs are provided by different estimators (function of the data) for attitude and position parameters based on a specific vision system (used to find relative position of a target). Philip and Ananthasayanam found that fixed gain observers were sufficient for estimation of position and attitude. They describe the sensitivity of different parameters for the estimators and controllers (flight controllers), and the range of parameters for which a successful maneuver towards the target can be achieved.

1.3 Autonomous In-Orbit Rendezvous

The first autonomous rendezvous, using relative GPS navigation, was performed by Engineering Test Satellite-VII (ETS-VII). Kawano, and Mokuno's paper (2011) (14) on optical navigation systems (degree of relative motion) for autonomous rendezvous docking explains the 1998 and 1999 unmanned autonomous rendezvous docking experiment. Performed successfully three times, it enabled highly accurate rendezvous and low-impact docking procedures. They used two optical navigation sensors which were the rendezvous laser radar and a proximity camera sensor. The optical navigation system and its design methods worked better than requirements during rendezvous docking experiments, and were applicable to future systems that aim to perform in-orbit servicing and planet explorer missions.

Henry and Zenteno-Torres (2021) (5) evaluated the potential of sliding-mode control and estimation techniques to address fault tolerance (ability to continue operating with component failure) against actuator faults (loss of controllability of a faulty actuator). The evaluation was for autonomous rendezvous between a chaser spacecraft (active and chases) and a passive spacecraft on a circular orbit. They utilized the dual quaternion formalism, which allows them to describe rotation and translational spacecraft dynamics in a single equation, as well as solar array flexible modes, propellant sloshing, and their coupling. They proposed a six degree-of-freedom fault tolerant control architecture, and an anti-windup strategy using polytope algebra. This prevents instability, and with intensive simulation the results demonstrate the fault-tolerant solution can cover any kind of thruster faults.

1.4 Specific In-Orbit Rendezvous Devices

Clerc, Renault, and Losa (2011) (3) researched the control of a magnetic capture device for autonomous in-orbit rendezvous. They explained the control aspects of the device used to return Mars soil samples to Earth. This mission involved a critical rendezvous phase and passive sample container that would be placed in Mars orbit by an ascent vehicle (two-stage solid-propellant rocket). The device needed to be reliable as well as simple in capture operations, which was achieved through damp rotation rates that enforce a relative orientation of the sample container at a range of four meters. To secure final contact, a small passive magnet was used.

Produced for the AAS and AIAA Conference (American Astronautical Society and American Institute of Aeronautics and Astronautics), Rajguru, Eyre, Ebrahimi, Barnhart, Griffith, Chibuzor, Haq, Nguyen, and Le (2022) (18) analyzed the optimization of RPO (Rendezvous and Proximity Operations) for assembly operations. This paper explains the benefits of the CLING-ERS in-orbit rendezvous device that combines RPO and Docking into a single module 4.

The CLING-ERS mechanism is highly compliant, has a low profile, can independently undock, not protruding, genderless, and uses Electronic Rendezvous Sensors embedded in its structure. CLING-ERS is highly compliant which allows docking under high positioning errors in all directions. The configuration of the docking tangs (in orange 4), allows for a swept cylindrical off-axis docking volume from internal angles. This design accommodates off-axis angles as shown in 5.

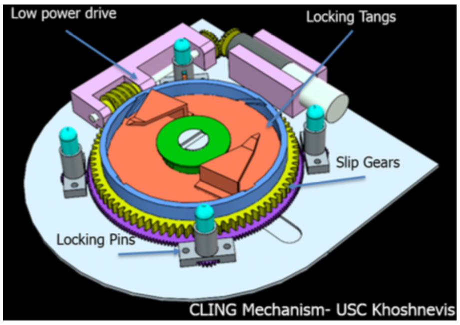

Figure 4: Original CLING-ERS Design: simple worm gear mechanism.

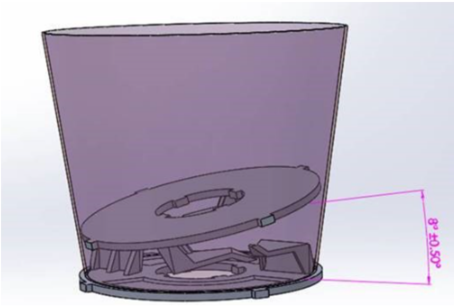

Figure 5: Angles of off-axis capabilities depending on specific “bend” of tines or fingers.

Several units of CLINGERS can be installed on multiple faces of a dockable surface of a space platform without enlarging the overall volume as the mechanism has a low profile. This is beneficial for docking in tight places where there are protrusions or a lack of volume. These modules can also independently disengage from docking even if one becomes non-responsive. CLINGER utilizes a unique genderless configuration, which allows for more maneuverability. Lastly, by using Electronic Rendezvous Sensors, as embedded for pose estimation, CLINGERS is able to relay range data and bear information to the host space platform.

1.5 CLING-ERS Rendezvous Proximity Operations

The CLING-ERS team is studying the effectiveness of implementing a RPO solution independent of the host’s navigational capabilities through the development of CLINGERS. The RPO experiment consists of two CLINGERS devices mounted separately to an Astrobee. In the first configuration both Astrobees are free flying. After activation of Bluetooth, each CLINGERS will query the other to determine relative location and pose before initiating the docking sequence. In the second configuration, one Astrobee is fixed to the ISS, so the free flying CLINGERS would be the “Servicer” in the scenario and the stationary CLINGERS would be the “Client”; a similar set of steps are carried out for docking.

The CLINGERS RPO algorithm is an autonomous program, which once initiated, will begin searching for the designated target, and go through a series of gateways 6a to accomplish docking.

CLINGERS utilizes three modes of information transfer to the host: providing raw sensor information to the host, providing processed range and bearing data to the host, and computing maneuvers for GNC (Guidance, Navigation and Control) to perform collaborative docking. CLINGERS finds its relative pose and position using the opposing CLINGERS’s IR LED lights, and a PNP (Perspective-n-Point) algorithm. CLINGERS sends the desired position or attitude to Astrobee, and does not directly command thrusters 7;. CLINGERS has no propulsion, therefore, all maneuvers are executed by Astrobee.

CLINGERS has two sets of LEDs 8 to provide perspective: far-field, and close-in site. Only one set of lights (outer or inner) will be active at a time. RPO starts once the outer lights are turned on. When the outer lights are occluded from the camera’s view, the inner lights are switched on. This allows for both far-field and near-field RPO with the same camera sensor.

1.6 Perspective-n-Point Algorithm

The Perspective-n-Point problem is one that has been attempted in multiple fashions by many researchers, with the ultimate goal of increasing accuracy and decreasing run time. A Perspective-N-Point Algorithm determines the pose (position and attitude) of the camera relative to some number n points in the 3D world, given the known position of

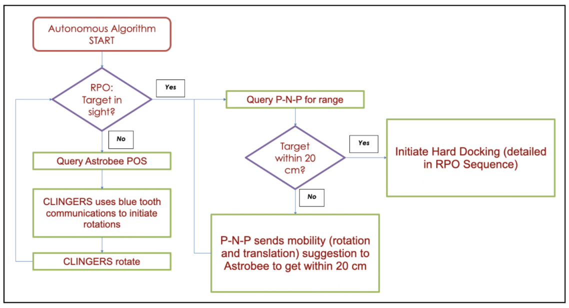

(a) The CLINGERS RPO algorithm includes a series of gateways, and is fully autonomous.

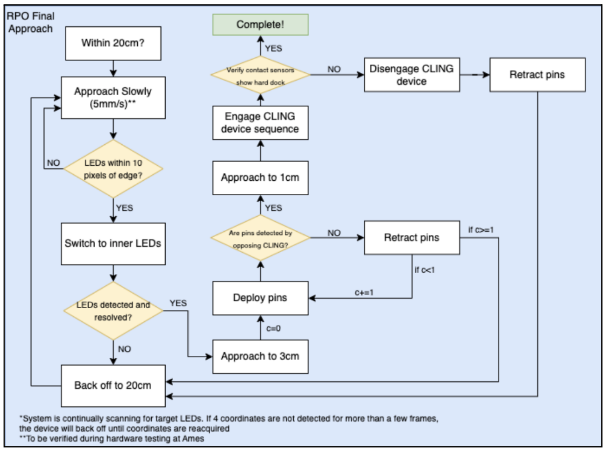

(b) Multiple safety gates are built into the RPO sequence.

Figure 6: RPO Algorithm and Sequence

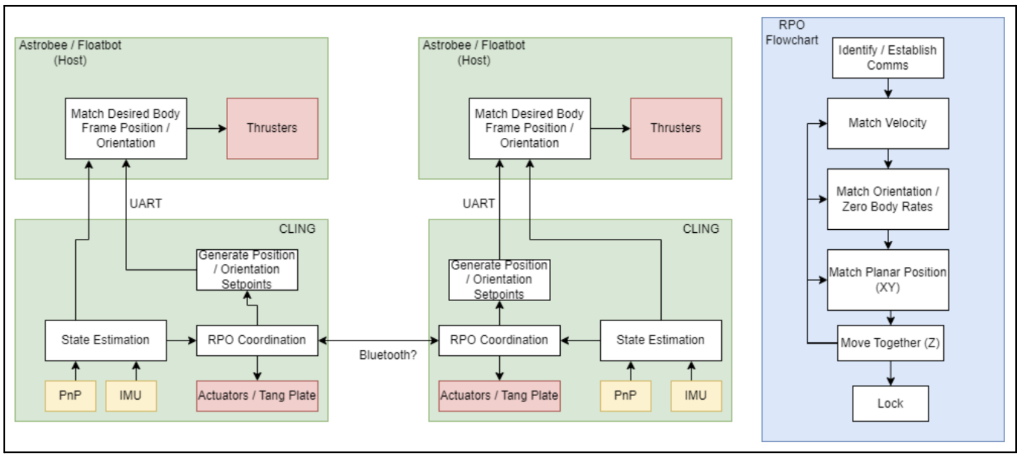

Figure 7: GNC Control Loop.

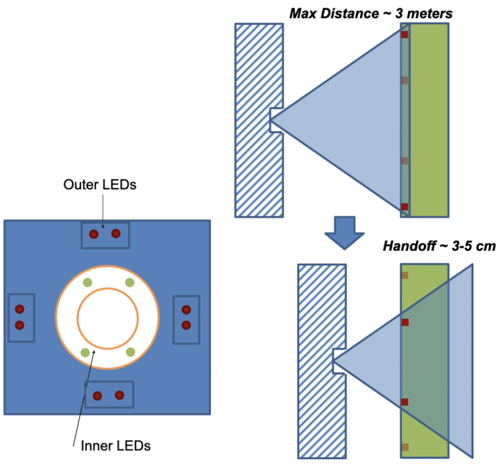

Figure 8: Configuration of outer and inner LEDs. Camera view in relation to distance and LEDs in use.

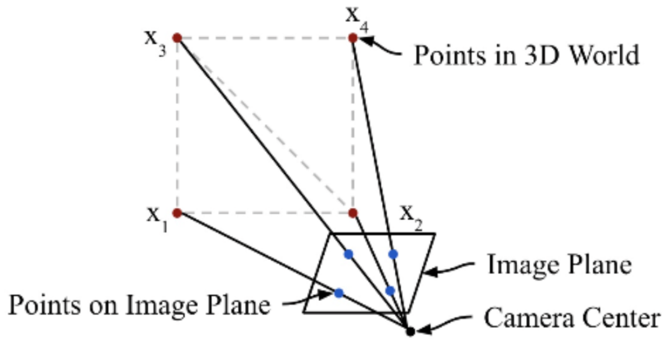

Figure 9: 3D coordinates, in relation to 2D pixel coordinates on an image plane, in relation to the camera center.

those points relative to each other in the 3D world and the corresponding pixel coordinates of those points on the camera's image plane9.

Lepetit, Moreno-Noguer, and Fua (2008) (12) found an accurate O(n) solution to the PnP problem. They proposed a non-iterative solution-estimating the pose of a calibrated camera from n 3D-to-2D point correspondences-which grows in computational complexity linearly with n. Contrasting the less accurate O(n^5) and O(n^8) solutions, their method is applicable for n being greater or equal to four, and handles planar and non-planar configurations. They express the n 3D points as a weighted sum of four virtual control points, and they solve for a small constant number of quadratic equations to pick the right weights. The output of the closed-form solution can be used to initialize a Gauss-Newton scheme, improving accuracy and using a negligible amount of additional time.

Another approach to the PnP algorithm by Hesch and Roumeliotis (2011)(6), utilized a Direct Least-Squares method in the general case of n being greater than or equal to 3. They formulated a nonlinear least-squares cost function based on camera measurement equations, that constitute a system of three third-order polynomials. After, they employ the multiplication matrix to determine roots for this system and minima without any iterations. This method is very scalable as the polynomial system is independent of the number of points.

1.7 Specific Perspective-n-Point Algorithms

Some of the lead approaches to the PnP problem include Nakano, Grafarend, Bujnak, Lu, Ke, Gao, Kneip and Banno's approach. Nakano's P3P approach (2019) (15) is what inspired CLING-ERS original P4P approach, and it utilizes an algebraic approach to the Perspective-n-Point problem. The distance from the camera center to the 3D points is represented by a rotation matrix, which then finds the distance by using orthogonal constraints of the rotation matrix. It has the second best performance against the state-of-the-art methods for both numerical accuracy and computational efficiency. It is both the fastest among quartic solvers and using a method similar to Banno's reduction of numerical operations, except this algorithm shows the issue P3P has with numerical stability as it has reported numerical degeneracy in the state-of-the-art methods for specific point-camera configurations.

Grafarend and Shan (1997)(4) also researched the PnP problem, and their paper solves the three-dimensional resection problem by at first computing the Cartesian coordinates of the perspective center using Möbius barycentric coordinates. They then represent them as space angles in a five-dimensional simplex, which is made using the unknown point and the four knowns. Unknown distances in the five-dimensional simplex are found using Grunert equations, through linear substitution and reduction to one equation.

Bujnak, Kukelova, and Pajdla (2008) (2) attempted the P3P and P4P problem where the focal length of the camera is unknown. Previously unsolved, they find the orientation determination of a camera with an unknown focal length and given images of four 3D reference points. They used a Göbner method basis to solve a system of polynomial equations using a hidden method.

Lu's (2018) (13) paper presents models to describe PnP problems, and introduces the P3P solution and the EPnP solution. The latter is used to reduce complexity by representing 3D points as a weighted sum of four virtual control points. They explain Gao et al and Wu-Ritt's zero decomposition method that provides a complete solution to the P3P problem.

Ke and Roumeliotis's (2017) (Ke) paper solve the perspective-3-point problem algebraically by determining the camera's attitude through employing geometric constraints. This formulates a system of trigonometric equations which are solved through an algebraic approach. Using this method the unknown camera position and rotation matrix can be found. This method is more numerically accurate at a low computational cost.

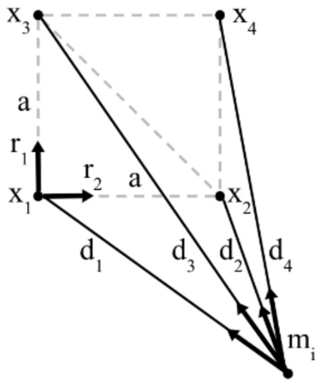

Figure 10: P4P Variables Representation: four 3D coordinates labeled X1-X4 have their corresponding pixel coordinates on the image plane, that are in relation to the camera center through vectors d1-d4.

Gao, Hou, Tang, and Cheng's (2003) (21) notable solution utilizes both an algebraic and geometric approach to the P3P problem. They use Wu-Ritt's zero composition algorithm to get a complete triangular decomposition solution. They also give explicit criteria for multiple solutions to the P3P problem. This is done in order to combine analytic solutions, and therefore provide an algorithm that can be used in robust numerical solutions.

Kneip, Scaramuzza, and Siegwart (2011) (11) proposed a new closed-form solution to the P3P problem, computing the aligning transformation in a single stage. This is done by introducing intermediate camera and world reference frames, and expressing their position and orientation using two parameters. Projecting the world point into a parameterized camera pose leads to two conditions and a quartic equation for finding four solutions for the pair. They are then substituted back to get camera poses in the world reference plane. The final algorithm is more lightweight than existing P3P-solutions and is also more accurate and precise at a lower computational cost.

Lastly, Banno (2018)(1) explains how his method starts from three similarity transformation equations that treat all extrinsic camera parameters in a vector of linear combinations. These transformation equations of the three coordinate pairs helped explain that all orientation parameters can be presented as a linear combination of six 15D vectors. The algorithm is found to be more accurate than Gao's method, of similar accuracy to Kneip's state-of-the-art method, and takes less time to run which allows for an advantage in running more hypotheses in a shorter amount of time.

1.8 CLING-ERS Nakano Inspired PnP

CLINGERS is utilizing a PNP algorithm to detect the "pose" of the other CLINGERS in relation to itself. It uses a single IR Camera and 4x IR LED lights on the target in order to detect the light and resolve its pose by translating and rotating to said target. Given the position of the points Xi relative to each other, and the corresponding pixel coordinates of each point on the camera's image plane, our algorithm finds the translation and rotation matrices between the camera coordinate frame and the coordinate frame centered on X1, where di defines the length of the projection rays from the camera center to each point in the 3D world 10.

The algorithm runs twice, once for points X1-X3 and once with points X2-X4, subsequently finding the true overlapping solution from the many P3P solutions. Finding d allows the derivation of t and R, the translation and rotation matrices which can be found by using the equation below.

$$p = \frac{1}{f} M_{inc} x_c \tag{1}$$

This equation shows the relationship between the pixel coordinates of the 2D projection of the image plane to the focal length, intrinsic parameters of the camera, and the 3D coordinates of the point on the image plane in relation to the camera center.

1.9 OpenCV PnP

Our team has also utilized OpenCV or Open Source Computer Vision to create another PnP algorithm (16) to solve the P4P problem more accurately. It uses a "solvePnP" function to estimate an object's pose in relation to direct points and their corresponding image projections, as well as the intrinsic matrix and distortion coefficients. In this orientation, the camera frame has the X-axis pointing right, the Y-axis pointing downwards, and the Z-axis pointing forwards 11.

The coordinates in the world frame are projected onto a 2D image plane using the perspective projection model II and the camera intrinsic parameters matrix (A or K). The estimated pose is therefore the rotation vector and the

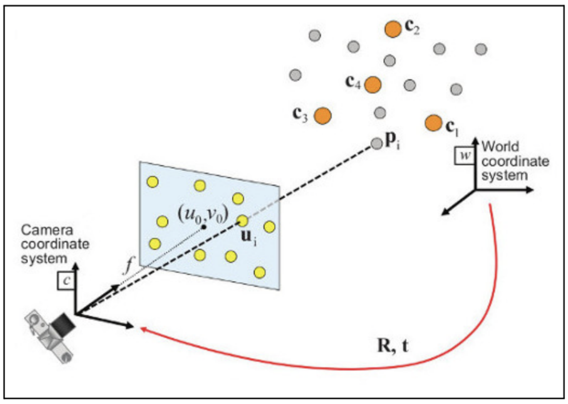

Figure 11: PnP Camera Frame Orientation: position of the camera coordinate system relative to the world coordinate system, where R and t are the rotation and translation matrices.

translation vector that transforms the 3D points in the world frame to the camera frame. The mathematical explanation for the points in the world frame projected into the image plane with translation and rotation vectors can be seen in the equations below.

$$\begin{bmatrix} u \\ v \\ 1 \end{bmatrix} = \boldsymbol{AII^{c}T_{w}} \begin{bmatrix} X_w \\ Y_w \\ Z_w \\ 1 \end{bmatrix} \tag{2}$$

$$\begin{bmatrix} u \\ v \\ 1 \end{bmatrix} = \begin{bmatrix} f_x & 0 & c_x \\ 0 & f_y & c_y \\ 0 & 0 & 1 \end{bmatrix} \begin{bmatrix} 1 & 0 & 0 & 0 \\ 0 & 1 & 0 & 0 \\ 0 & 0 & 1 & 0 \end{bmatrix} \begin{bmatrix} r_{11} & r_{12} & r_{13} & t_x \\ r_{21} & r_{22} & r_{23} & t_y \\ r_{31} & r_{32} & r_{33} & t_z \\ 0 & 0 & 0 & 1 \end{bmatrix} \begin{bmatrix} X_w \\ Y_w \\ Z_w \\ 1 \end{bmatrix} \tag{3}$$

$$\begin{bmatrix} X_c \\ Y_c \\ Z_c \\ 1 \end{bmatrix} = \boldsymbol{^{c}T_{w}} \begin{bmatrix} X_w \\ Y_w \\ Z_w \\ 1 \end{bmatrix} \tag{4}$$

$$\begin{bmatrix} X_c \\ Y_c \\ Z_c \\ 1 \end{bmatrix} = \begin{bmatrix} r_{11} & r_{12} & r_{13} & t_x \\ r_{21} & r_{22} & r_{23} & t_y \\ r_{31} & r_{32} & r_{33} & t_z \\ 0 & 0 & 0 & 1 \end{bmatrix} \begin{bmatrix} X_w \\ Y_w \\ Z_w \\ 1 \end{bmatrix} \tag{5}$$

The ultimate goal for the CLING-ERS project as a whole, is to validate the benefits of merging multiple RPOD functions into a single element. The basic system has been demonstrated on the ground in a 2D testbed. The final testing, inside the ISS laboratory, will prove the concept in full 6DOF. Currently the privatization of the space industry has created a boost of commercial launch vehicle companies that are reducing the cost of launch mass. The benefit of having the capability of modular spacecraft aggregating in orbit can go hand in hand with the current trends in this industry. CLINGERS' performance capabilities have been validated in 2D at a system level. For full validation, successfully demonstrating autonomous docking and undocking of CLINGERS, in a 3D setting and in microgravity, is next.

2 Methods and Results

The CLING-ERS flight hardware assembly was completed in 2022, and flight hardware testing occurred in January and February of 2023. From the summer of 2022 to the months leading up to the end of 2022, there were copious amounts of testing performed in order to solidify our algorithm, as well as gain approval from NASA to continue on to the next Phases of the project.

Through this testing we improved our mechanical design, changed our PnP algorithm from a Nakano inspired PnP to an OpenCV based one, and solidified results for our RPO sensing program. As we prepared for the planned launch of the CLING-ERS units in June of 2023, we continued to perform testing on the static test stand with Float Bots, as well as testing at NASA's AMES Research Center (more authentic zero-gravity conditions).

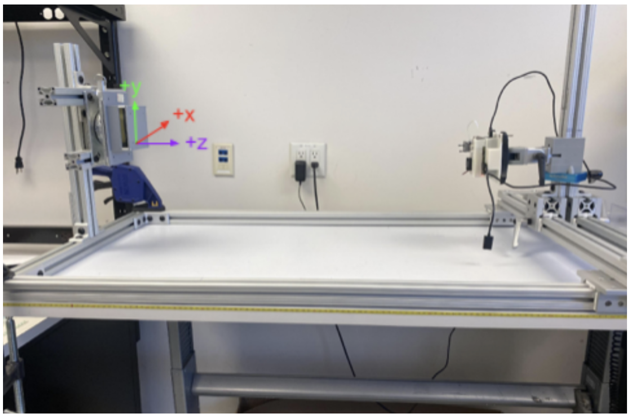

Figure 12: Static Test Stand containing an LED board with 4 IR LEDs and a Raspberry Pi 4 Camera.

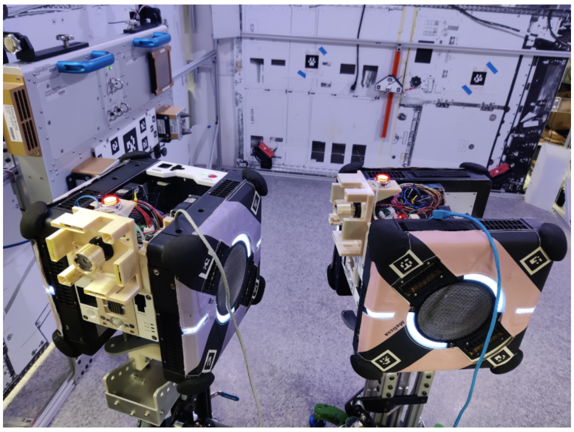

Figure 13: Dynamic Testing: NASA Ames. CLING-ERS mechanisms tested with Astrobee.

2.1 Initial Static Test Stand Testing Of Nakano PnP

In order to validate the various functions of our unit, we have taken a stepwise approach to testing in 2D static and dynamic testbeds. Our static test stand 12 was built to accommodate both translational and rotational orientation thru sliders and a positioning arm with 2 degrees of freedom (yaw and pitch), and a turntable (roll), to provide known position and pose to validate the PnP algorithms.

The Nakano Inspired PnP algorithm was tested for $\pm$ X translation, $\pm$ Y translation, +Z translation, $\pm$ X and yaw, $\pm$ Y and pitch, and + Z and roll. For each trial five data points were taken and the differences in measurements and output PnP data were calculated. Overall we found translation to be relatively accurate, with the Max Delta ranging from 0.2-4.09 cm. However, when it came to testing rotation the Max Yaw Delta was 6.8 degrees, while the Max Pitch Delta was 9.14 degrees and the Max Roll Delta was 28.5 degrees. These were significant inaccuracies, and a potential source of error is that when the orientation angle of the camera is increased, the LED blobs sensed become more oval than circular, and when we find the coordinates (i.e. finding the centroid), we might acquire coordinates that don't correspond to the actual location of the LED.

2.2 First Dynamic Testing At NASA's AMES Research Center

In the first week of December 2022, we performed dynamic testing of CLING-ERS units in NASA's Ames Research Center 13.

During testing we established communication with Astrobee and made sure the CLINGERS mechanical and electrical systems were compatible. We also validated the Nakano inspired PnP translation, however, rotation was not able to be verified. On the first day, the CLINGERS EDU V1.0 was test fitted onto the Astrobee demo platform, the coordinate system for PnP was changed meaning the order of the LEDs went anti-clockwise, and USB connection was found to be successful. We also realized extra LEDs on Astrobee could potentially be detected and throw off our PnP solution. On day two we conducted electrical tests, calculated distances between LEDs, fixed communication issues introduced by switching to syncWrite and syncRead on the android app, and successfully sent a message from RPi to Astrobee after an app rewrite, validating communications.

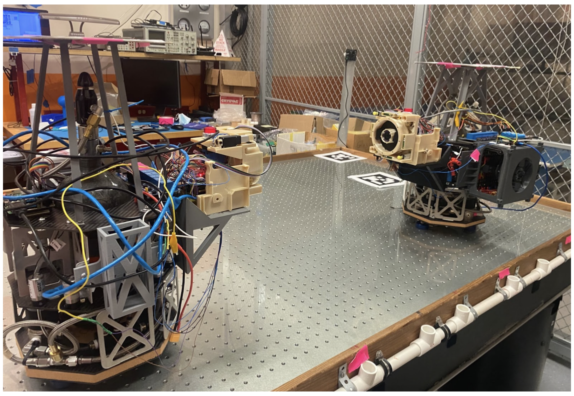

Figure 14: Two CLINGERS mounted onto separate Float Boats to perform docking.

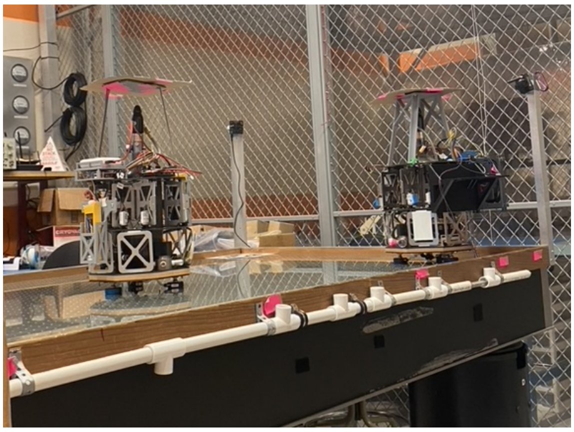

Figure 15: February 2023 Float Bot testing.

2.3 Initial Dynamic Environment and RPO Validation Float Bot Testing December 2022

After testing at the Ames Research Center where we had control on a floating platform in the Astrobee configuration, we continued testing on SERC's Air Bearing Platform 14, which is near frictionless and has Floatbots that can host CLINGERS and begin to validate an actual approach rendezvous and then contact to dock. It can demonstrate the movement of RPO between two CLINGERS enabled Floatbots, allowing for devices to be in a single plane for easy verification and modification of RPO testing. As the Nakano inspired PnP was producing inaccurate results, we transferred over to an OpenCV PnP algorithm.

In order to test CLINGERS on the Float Bots, we had to calibrate the Floatbot locations by moving them to various positions around the table and recording the measured position and angle from the camera to the true position. The testing that followed was a careful and exact process, where measurements were taken to approximately the nearest one and a sixth millimeter in order to maintain accuracy of our PnP. At each data point 3 rotational measurements were taken, at 0, 30, and 60 degrees on an evenly spaced 3x4 grid. We then calculated the relative pose OpenCV produces, and based on what Astrobee produces, we compared our PnP data to determine our accuracy.

2.4 February of 2023 FloatBot Testing

The FloatBot testing 15 is 1g ground dynamic testing performed on an air bearing platform. These FloatBots are placed on a single plane, and have 3 Degrees of Freedom (Limited Contact Dynamics) (19). The test campaign validates the overall RPO sequence, which includes the Astrobee communications handshake. This is not the final set of testing, as it does not validate CLINGERS performance in the z direction and pitch and roll rotations; however, we planned to perform further testing, to validate the initial RPO software variables, before the launch of CLINGERS to the ISS on June fifth, 2023.

For testing procedures one EDU unit must be tested using the dynamics from one Floatbot to validate communication requests from the RPi to the Floatboat, and that basic initial RPO functions can drive the Host. The second float serves as a static inert platform that provides a platform for a second CLINGERS unit but does not have propulsion capability. We validated communication from USB to Rpi to simulate the data transfer across the Astrobee connector to Astrobee. We ran tests to show initial RPO requests a move to a location of the Floatbot (acting as the host and

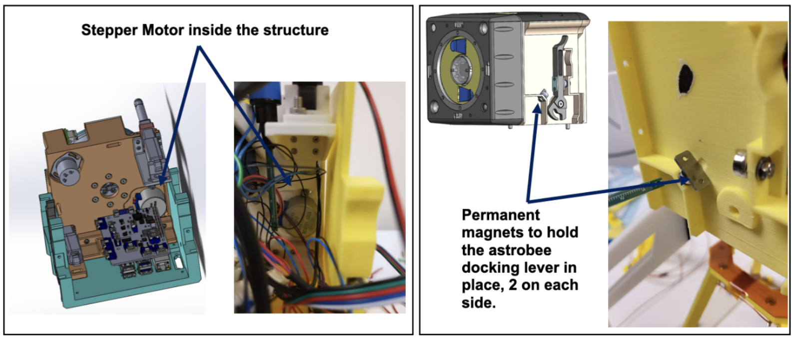

Figure 16: Magnetics: CAD file comparison to actual Stepper Motor and depiction of magnet location for docking lever.

Object	Distance	Gauss Reading
Side Magnet and Locking Lever Magnet	1 cm	6.3
	4 cm	1
	7 cm	**0.6**
Stepper Motor	1 cm	1.2
	4 cm	1.3
	7 cm	**0.4**

Note: Higher reading at 4cm for stepper motor due to sensor in proximity of the two external lever magnets

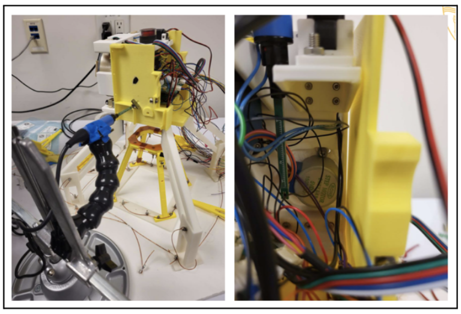

Figure 17: Magnetic Testing: Gauss testing results and depiction of Gauss Meter testing of magnets.

Proxy to Astrobee), and then the Floatbot uses its overhead inertial navigation to move to a requested point on the table. We tested the ability for an Ethernet connection to actively replace the Master-Scheduler.py code on the Raspberry Pi, in the same manner as may be needed on orbit. This required the CLING unit to be powered on and have entered the correct boot sequence. We also provided that a single laptop with either ethernet cable, can upload a new Master-Scheduler.py file, and then cycle power.

2.5 EDU Assembly Process

We needed two full flight units to be assembled. The assembly process included creation of a Bill of Materials, before sorting specific parts into stages of assembly, and division of work. CLINGERS was calculated to have a mass of 1155.9 g, and 1271.5 g with 10 percent contingency.

This process required 3D parts, fasteners and an installation of the ethernet connector in the Fan Plate and retrofit after delivery to USC. We also completed the assembly of the PCB (Printed Circuit Board) and prepared it for testing. We made sure that each flight unit had the most recent Master-Schedule.py code on it, and a revision system in place for that code. Adhering to careful procedures during assembly was vital as afterwards there was a basic run of each flight unit, checking the functions of the RPO (Rendezvous and Proximity Operations): power on, lights check, tang plate rotation, actuator extension and retraction. We meticulously worked to make sure the assembly was both thorough and clean by using protection, sanitizing materials, and performing the assembly in a class 100k cleanroom.

2.6 Magnetic Testing and Fan Safety

There are two sets of magnetic elements on CLINGERS: Stepper Motor with permanent magnets, the Astrobee adaptor chassis (total of four magnets per unit).

We performed magnetic testing to assure acceptance of these magnets by NASA in the upcoming Safety Review. Per ISS Regulations each magnetic element should be less than 3.16 Gauss as measured at seven cm. After further testing with a Guassmeter at different distances to both magnetic elements, we concluded our magnets complied with DC magnetic field requirements.

CLINGERS also utilizes a dual fan cooling system; the top fan brings air in while the bottom draws air out. To assure safety for astronauts, we installed a nylon safety mesh to cover the access of the fan from the outside, and the entrance to the fan on the inside of the device. The external cover allows safety if contact is to be made with the spinning fan, while the internal mesh prevents potential ingestion of any debris.

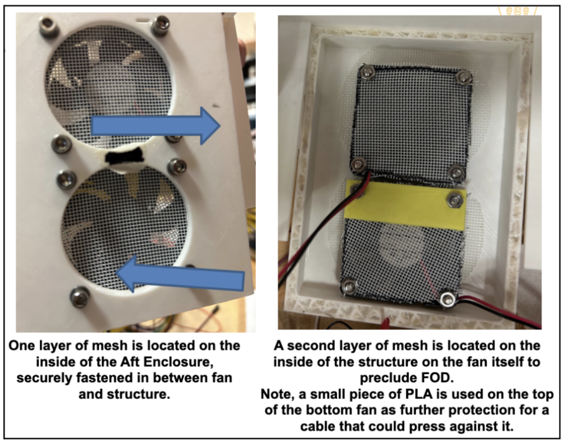

Figure 18: Fan Safety Mesh Installation: locations and expected air flow from fans.

Upon I and T testing, it was discovered the external facing mesh could easily be pushed, such that it would rub the fan while running. These were not the preferred operating conditions, as the fan did continue to run, but it was very loud. To prevent this deformity upon applied pressure, we placed a small spacer between mesh and fan to allow for deformation of mesh on the inside.

2.7 Wifi Analysis and Electronic Testing

The WiFi on the Raspberry Pi 4B was software disabled when the CLING-ERS units were launched to the ISS. The transmitter Chip that is in use on the Raspberry Pi 4B is the same one for both Wifi and BT. The Radio Frequency Hazard Calculator Analysis was validated at the frequencies of both WiFi and BT frequencies. We found BT frequencies of 2402 to 2480 mega hertz, and WiFi frequencies of 2401 to 2473 mega hertz, which led us to the conclusion that this would not be a possible hazard.

Electronic testing of CLINGERS was still in progress at the time, but the functional validation was already complete. We planned to do the following when testing the electronics. First, the safe to mate harness test. This means no continuity from each power rail (Vin, 5V,3.3V, LED 3.3V line) to ground and to each other, and checking for continuity on each rail/cable. We must also check for wiring errors that could apply over voltage, reverse polarities, and conduct this test on the Astrobee connector. The completed functional validation was confirming the Pi turns on to desktop, actuators can be moved forward and reversed, Stepper motor can be moved in both directions, ADC can read encoder and reflectivity sensors, and LED controller can turn on each LED string individually. For emission checks, we planned to check ringing on the buck converter switch net, make sure RF profile validation meets ISS requirements, and perform the EMI/EMC compatibility test. We planned to perform a thermal test using a thermocouple to measure temperatures on the buck converter IC and check if it heats up. Finally, we planned to perform a vibration test to check that all connections can withstand the described vibe profile.

2.8 Data Flow and Data Flow Testing

CLINGERS continuously communicates back and forth with Astrobee in order to execute its RPO sequence. This also means CLINGERS will have to communicate, occasionally, with the other CLINGERS via bluetooth. RPO data will be transmitted through a wireless bluetooth connection between the two CLINGERS. In any operation, there will also be continuous data flow between CLINGERS and its host: Astrobee.

This occurs through CLINGERS interfacing with Astrobee's High Level Processor (HLP) which runs on a custom Android OS. Modes one and two of information transfer require CLINGERS to be sending data to Astrobee while CLINGERS Guest Science Android App (APK) gathers data. Finally, in mode three, the CLINGERS APK will act as an intermediate between the CLIGNERS RPO algorithm and the Astrobee GNC; it will take in GNC recommendations from the CLINGERS and execute them in Astrobee. All transferred data will be formatted as a notarized JSON (JavaScript Object Notation), which is strong for simple processing.

After establishing these data flow pathways, we began testing these systems. We used a mixture of hardware and simulation tools to recreate the environment with Astrobee. A 6640 board, inforce, is used as a "Development HLP" for hardware testing. The Inforce interfaces with NASA ARC's Astrobee Simulator Software to test trajectories and Astrobee operations. An RPi 4b can be connected to the USB port on the Inforce to test serial communications between the two boards, and bluetooth testing will occur between two RPi 4bs. The complete plan for this testing involved sending sample string from RPi to inforce, sending JSON strings and parse JSON in inforce, sending and parse JSON and sending telemetry back from inforce, NASA ARC Test one of full CLIGNERS and Astrobee Communications,

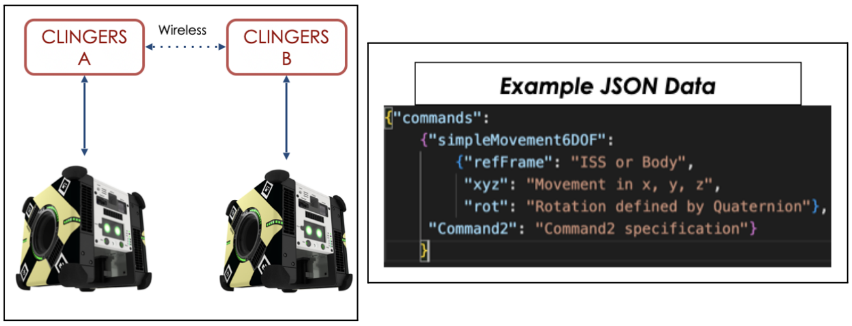

Figure 19: Data flow between each CLINGERS. JSON (JavaScript Object Notation) example Data.

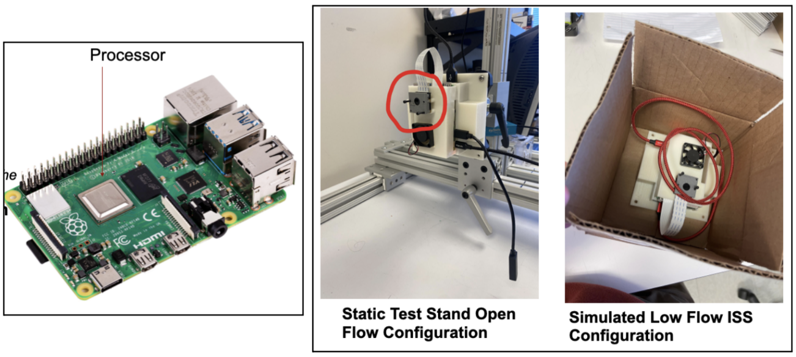

Figure 20: Touch Temperature Validation and Raspberry Pi 4B Thermal Testing.

sending simple string from RPi to RPI with bluetooth, sending and parse JSON string from RPi to RPi with bluetooth, and finally, full serial and bluetooth testing with two RPis and inforce.

2.9 Environmental Testing

Given the fast pace of the mission no environmental testing is planned. EMI testing was done by NASA MSFC on the Raspberry Pi 4B as it is the first one to be launched and flown inside the ISS.

2.10 Raspberry Pi Thermal Testing

There is only one component inside CLINGERS that generates heat and requires validation, and it will not drive external structure over Touch Temperature limits. To confirm this, we performed a Touch Temperature validation. We confirmed all CLINGERS electronics will not be exposed to any crew during operation, and we planned to do Touch Temperature tests on the EDU unit once it was assembled to validate our predictions. The only component that does heat is the Raspberry Pi 4B; we do however, have internal fans to provide airflow over the processor, which happens to shut down until onboard temperatures fall below 60 degrees celsius.

We performed internal Raspberry Pi 4B testing for a heat load. We wanted to validate this testing, and before structural touch temperature the team did testing of the component that gets the hottest inside the CLINGERS Unit. Two different Configurations were used to test the Pi thermal load: Static Test Stand with OpenFlow Configuration, Simulated CLINGERS encapsulated with single Fan.

The internal thermal was done in Ambient with different configurations and conditions, and our thermal data was taken from the onboard temperature sensor from the CPU. For the setup of our fourth test is the most ideal case for the Raspberry Pi remaining at the lowest temperatures possible while running software. Furthermore, a heatsink was already installed on the Pi prior to the thermal testing. We found favorable results with temperatures remaining at desired levels for the expected ISS configuration.

2.11 Phase II/III Safety Review

The Phase II/III Safety Review on March ninth, 2023, was a great success. The CLING-ERS team presented the project along with completed safety testing and analysis, and detailed descriptions of each mechanism. Updates for this safety review included Astrobee Adaptor changes, no caps on the end of Linear Actuators, enlargement of TPU bumpers on aft, addition of ethernet thru connection, and much more.

Both Fans Functioning							
	Side (as viewed from docking mechanism)						
Time (min)	Front	Top	Left	Right	Back	Bottom	Internal
0	20.3	20.2	20.4	20.3	20.6	20.6	37
1	20.7	20.5	20.6	20.4	20.4	20.7	51
2	21.2	20.8	21	20.9	20.7	21.3	52
3	21.5	21.2	21.4	21.2	21.2	22	54
4	21.7	22.1	21.5	21.4	21.3	22.6	54
5	21.8	21.7	21.8	21.8	21.4	22.6	55
6	22	21.7	22.1	21.7	21.4	22.6	55
7	22.2	21.9	22.2	21.8	21.8	23.1	54
8	22.2	22	22.2	22.1	21.9	23.3	55
9	22.3	22.2	22.3	22.2	21.7	23.6	54
10	22.4	22.2	22.6	22.3	22	23.5	55
11	22.4	22.6	22.7	22.5	22.3	23.7	55
12	22.7	22.6	22.9	22.6	22.6	23.8	55
13	22.8	22.8	22.9	22.8	22.5	24	54
14	22.9	22.8	23.1	23.1	22.5	24.1	55
15	23.1	22.9	23.2	22.8	22.8	24.2	55

One Fan Functioning							
	Side (as viewed from docking mechanism)						
Time (min)	Front	Top	Left	Right	Back	Bottom	Internal
0	21.4	21.3	21.4	21.5	22	22.4	39
1	21.3	21.2	21.3	21.3	22	21.6	52
2	21.6	21.1	21.4	21.4	22.1	21.9	54
3	22	21.3	21.9	21.6	22.4	22.3	56
4	22.3	21.6	22.4	21.8	23.2	22.9	56
5	22.7	22.1	22.6	22.3	23.3	23.2	57
6	22.7	22.2	22.7	22.2	23.3	23.6	58
7	22.7	22.4	22.6	22.5	23.6	23.8	58
8	23.3	22.6	23.2	22.9	24.4	24.3	59
9	23.3	22.9	23.2	22.9	24.1	24.6	58
10	23.5	23.1	23.5	22.9	24.4	24.6	58
11	23.6	22.8	23.3	22.8	24.5	24.7	59
12	23.2	22.7	23.4	23.1	24.7	24.9	58
13	23.4	22.9	23.4	23.1	24.5	24.7	59
14	23.3	22.9	23.6	23.2	24.4	25	59
15	23.4	22.9	23.4	23.2	24.2	25	59

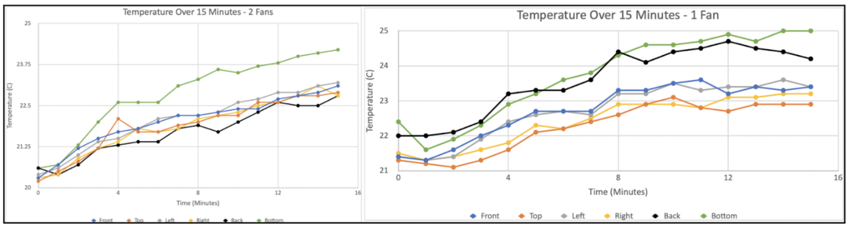

Figure 21: Raspberry Pi internal thermal test results and graphs under different configurations and conditions.

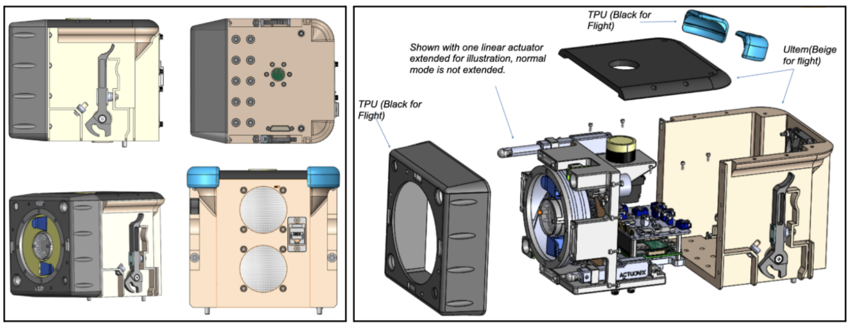

Figure 22: Self-contained CLING-ERS unit and mechanical exploded view of full model.

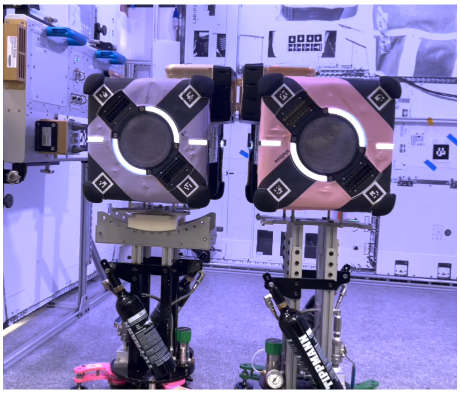

Figure 23: CLINGERS near docking on the granite table.

At the end of the review, the chair gave final approval with no modifications, pending Professor Barnhart's final inspections. This success was due to the meticulous and tireless work of the CLING-ERS team, as well as the solid design and analysis test process.

2.12 Second NASA's AMES Research Center Testing May First and Second

The second NASA Ames trip was estimated to occur in April-May of 2023. Before the team was ready for testing, there was work done in regards to software. This included further bluetooth communication between CLINGERS units and work on logging and data storage on Astrobee. Additionally, we needed to integrate all of these parts together. During this trip we wanted to validate the accuracy of EKF state estimation to within xx cm and yy deg in three degrees of freedom at a wide variety of ranges and orientations, validate the ability of CLINGER to guide astrobee to various poses relative to both a stationary and moving CLINGERS, validate the ability of RPO algorithm to dock CLINGERS in three degrees of freedom, and validate the soft-start capability using host position information. Testing at AMES with a 6 DoF Lab would enable full end-to-end verification of the RPO sequence, with the CLING-ERS module integrated into, and communicating with, the Astrobee host for the duration of the test.

The team went on the second NASA Ames trip on May first and second. The testing that occurred on the first day included confirming bluetooth communications from CLINGERS to Astrobee, API integration, confirming UART communications, and basic APK testing. On the second day the team connected to CLINGERS with Ethernet in order to get the correct IP address to connect to the Pi using a computer and VNC Viewer. The team then tested the PnP program and took measurements of where the CLINGERS were distance wise from each other, and how that corresponded to what PnP gave as the CLINGERS location, which was found to be very accurate.

On the first docking attempt CLINGERS docked successfully after the docking sequence itself ran twice until the tangs interlocked and the CLINGERS docked fully. However, when testing whether everything would work together, meaning both RPO and docking, the team was not able to confirm success during the trip. One issue observed during testing was the loose connection of the cooling fan connector to the PCB, because if the fans stop working RPi cannot continue to operate. The team then worked towards finding a solution for this threat.

2.13 Third NASA's AMES Research Center Testing May Twelfth

The team decided to take another trip to NASA's Ames Research Center in an attempt to confirm the full RPO and docking sequence on the granite table. This trip however, was unfortunately unsuccessful. The EDUs were not able to communicate with Astrobees or a computer by USB. The UART to USB conversion takes place on the custom PCB board and is then connected to the CLINGERS' Astrobee connector. We did not know whether the UART to USB chip on the custom board was malfunctioning or if the board itself had issues, or if there was a bad connection between the wires and the connectors that connect the board (like the cooling fans) etc. These problems were not present during EDU testing on May first and second. Everything else including power, sensors, actuators, and RPi were working. Both EDUs were found to have the same failure.

3 Discussion

The CLING-ERS project is improving autonomous In-Orbit Rendezvous and docking in space, with the overall goal of increasing accuracy and safety in RPO scenarios between two objects. This will allow for semi-standard mechanical equipment standard docking methodology with an optimized passive capture technique mechanism and Open Source PnP algorithm.

3.1 Purpose and Significance of Results

The impact of CLING-ERS will be felt among engineers who will be able to take a more flexible approach to docking system for large scale assembly in space. The CLING-ERS mechanism will also improve Rendezvous and Proximity Operations for two spacecraft, allowing for efficient spacecraft servicing, repair, maintenance, and even potentially self-propagation.

3.2 Project Limitations

As previously stated, given the fast pace of the project no environmental testing was performed, and EMI testing was done by NASA MSFC on the Raspberry Pi 4B as it is the first one to be launched and flown inside the ISS.

After initial Static Test Stand testing of the Nakano based P4P algorithm, the team made the decision to switch to an Open Source PnP algorithm to assure accuracy; CLING-ERS is currently using this OpenCV algorithm.

3.3 Future Directions

CLING-ERS will perform further testing at NASA's Ames Research center to confirm success of the RPO and docking sequence utilizing a PnP algorithm. CLINGERS launched to the ISS on June fifth, 2023 with the SpaceX CRS-28 mission.Tthe two CLINGERS will be tested on the ISS in late 2023, and will be attached to separate Astrobee's where they will dock in 3D by utilizing an internally developed PnP (Perspective-n-Point) algorithm that allows the pinpoint of LEDs on the CLINGERS which then transmits pose and range information (orientation and distance) to the Astrobee hosts. The Astrobee then can rotate and translate to the other CLINGERS to prove docking. Future Ames testing will allow CLING-ERS to determine the viability of our docking mechanism in real space conditions, and if effecient and accurate docking is accomplished in the ISS, the CLINGERS mechanism will have been successful.

References

[1] Banno, A. (2018). A p3p problem solver representing all parameters as a linear combination. *Image and Vision Computing*, 70:55–62, DOI: https://doi.org/10.1016/j.imavis.2018.01.001.

[2] Bujnak, M., K. Z.-. P. T. (2008). A general solution to the p4p problem for camera with unknown focal length. *2008 IEEE Conference on Computer Vision and Pattern Recognition.*, DOI: https://doi.org/10.1109/cvpr.2008.4587793.

[3] Clerc, S., R. H.-. L. D. (2011). Control of a magnetic capture device for autonomous in-orbit rendezvous. *IFAC Proceedings Volumes*, 44(1):2084–2089, DOI: https://doi.org/10.3182/20110828-6-it-1002.01499.

[4] Grafarend, E. W., . S. J. (1997). Closed-form solution of p4p or the three-dimensional resection problem in terms of möbius barycentric coordinates. *Journal of Geodesy*, 71(4):217–231, DOI: https://doi.org/10.1007/s001900050089.

[5] Henry, D., Z.-T. J. C. J. F. D. L.-A. . D. J. (2021). A 6-dof sliding mode fault tolerant control solution for in-orbit autonomous rendezvous. *Aerospace Science and Technology*, 118:107050, DOI: https://doi.org/10.1016/j.ast.2021.107050.

[6] Hesch, J. A., . R. S. I. (2011). A direct least-squares (dls) method for pnp. *2011 International Conference on Computer Vision.*, DOI: https://doi.org/10.1109/iccv.2011.6126266.

[7] Institute., I. S. ((n.d.)a). Space engineering research center. *Retrieved October 21, 2022, from*, https://www.isi.edu/centers-serc/research/rendezvous-and-proximity-operations-rpo/cling-and-clingers/.

[8] Institute., I. S. ((n.d.)b). Space engineering research center. *Retrieved October 21, 2022, from*, https://www.isi.edu/centers-serc/research/rendezvous-and-proximity-operations-rpo/.

[9] Kanis, S. (2016, November 8). What is astrobee? *NASA. Retrieved December 19, 2022, from*, https://www.nasa.gov/astrobee.

[Ke] Ke, T. An efficient algebraic solution to the perspective-three point problem. *2017 IEEE Conference on Computer Vision and Pattern Recognition (CVPR).*, DOI: https://doi.org/10.1109/cvpr.2017.491.

[11] Kneip, L., S. D. a. S. R. (2011). A novel parametrization of the perspective-three-point problem for a direct computation of absolute camera position and orientation. *CVPR 2011.*, DOI: https://doi.org/10.1109/cvpr.2011.5995464.

[12] Lepetit, V., M.-N. F. . F. P. (2008). Epnp: An accurate o(n) solution to the pnp problem. *nternational Journal of Computer Vision*, 81(2):155–166, DOI: https://doi.org/10.1007/s11263-008-0152-6.

[13] Lu, X. X. (2018). A review of solutions for perspective-n-point problem in camera pose estimation. *Journal of Physics: Conference Series*, 1087:052009, DOI: https://doi.org/10.1088/1742-6596/1087/5/052009.

[14] Mokuno, M., . K. I. (2011). In-orbit demonstration of an optical navigation system for autonomous rendezvous docking. *Journal of Spacecraft and Rockets*, 48(6):1046–1054., DOI: https://doi.org/10.2514/1.52193.

[15] Nakano, G. (Retrieved December 11, 2022, from). A simple direct solution to the perspective-three-point problem. *Perspective-N-point (PNP) pose computation. OpenCV. (n.d.).*, https://docs.opencv.org/4.x/d5/d1f/calib3d_solvePnP.html.

[16] (n.d.)., O. (Retrieved December 11, 2022, from). Perspective-n-point (pnp) pose computation. https://docs.opencv.org/4.x/d5/d1f/calib3d_solvePnP.html.

[17] Philip, N. K., . A. M. R. (2003). Relative position and attitude estimation and control schemes for the final phase of an autonomous docking mission of spacecraft. *Acta Astronautica*, 52(7):511–522, DOI: https://doi.org/10.1016/s0094-5765(02)00125-x.

[18] Rajguru, A., Ebrahimi, E., Barnhart, D., Adam, H., Griffith, T., and Haqi, S. (2022). Clingers: Optimizing rpo ease for assembly operations. In *IAA SYMPOSIUM ON SAFETY, QUALITY AND KNOWLEDGE MANAGEMENT IN SPACE ACTIVITIES*, volume IAC-21,D5,1,8,x65885.

[19] Rughani, R., V. L. . B. D. A. (2019). Swarm rpo and docking simulation on a 3dof air bearing platform.

[20] Wertz, J. R., . B. R. (2003). Autonomous rendezvous and docking technologies: status and prospects. *SPIE Proceedings*, DOI: https://doi.org/10.1117/12.498121.

[21] Xiao-Shan Gao, Xiao-Rong Hou, J. T. . H.-F. C. (2003). Complete solution classification for the perspective-three-point problem. *IEEE Transactions on Pattern*, DOI: https://doi.org/10.1109/TPAMI.2003.1217599.